sciendo

*PRODUCTION ENGINEERING ARCHIVES* 2023, 29(1), 44-57

*PRODUCTION ENGINEERING ARCHIVES*

ISSN 2353-5156 (print)
ISSN 2353-7779 (online)

Exist since 4th quarter 2013
Available online at https://pea-journal.eu

# Automated Design of Honeycomb Conformal Cooling Channels for Improving Injection Molding Quality

**Yuan-Ping Luh[1], Chien-Chuan Chin[2], Hong-Wai Iao[1*]**

[1]College of Mechanical and Electrical Engineering, National Taipei University of Technology, Taipei City, Taiwan (R.O.C); yuan@mail.ntut.edu.tw (YPL); davidchin0910@gmail.com (CCC); iao.hongway@gmail.com (HWI)
[2]Graduate Institute of Manufacturing Technology, National Taipei University of Technology, Taipei City, Taiwan (R.O.C)
*Correspondence: iao.hongway@gmil.com

**Article history**
Received 10.10.2022
Accepted 21.11.2022
Available online 20.02.2023

**Keywords**
Conformal Cooling Channel
Automatic Constructed
One-Mold-Multiple-Cavities
Cold Runner System
Honeycomb

**Abstract**
The study of conformal cooling channel usually has adopted two assumptions in model design: the use of (1) a hot runner system and (2) a one-mold-one-cavity design. These assumptions substantially simplify the research. However, most molds are designed using a cold runner system and multiple cavities. These two assumptions may not apply to all commercial systems; hence, a design method for honeycomb CCCs for cold runner systems and multiple cavities is proposed in this study. Specifically, an algorithm was developed to automatically design CCCs for such systems. This algorithm can be used to reduce the cooling time, improve product quality, and ensure that the system temperature is relatively homogenous in practical situations. According to the result of this study, the honeycomb CCC models were more effective at maintaining a homogeneous temperature distribution, reducing shrinkage, and reducing warpage for both parts produced from the same two-cavity mold, thus ensuring consistent part quality.

DOI: 10.30657/pea.2023.29.7

## 1. Introduction

Injection molding is one of the most effective methods for producing large quantities of plastic parts, and various injection molding methods have been developed and applied in the manufacturing industry, including gas-assisted injection molding, insert molding, and microcellular molding. All injection molding methods involve the processes of filling, packing, and cooling. In the filling process, the plastic melt is rapidly injected into the mold cavity. In the packing process, the melt is compressed until its surface becomes frozen, producing the desired shape. Finally, in the cooling process, excessive heat is quickly removed from the melt and mold, reducing the molding cycle time and improving product quality. Scholars have estimated that the cooling process accounts for 40%–70% of the total molding cycle time (Li et al., 2005; Hus et al., 2013). Therefore, reducing the cooling time can effectively reduce the molding cycle time.

Cooling performance affects both production capacity and quality. A mold is essentially a heat exchanger; the melt introduces heat into the mold, and a cooling system removes excessive heat. Mold cooling systems leverage both conduction and radiation to transfer heat to fluid in cooling channels for removal. Park and Kwon (1998) examined the heat dissipation efficiency of cooling systems for injection molding and concluded that the heat dissipation efficiency of the mold itself is only 5%, whereas cooling channels remove 95% of the heat in the mold. Therefore, improving the cooling channel design can reduce both the molding cycle time and improve product quality. Typical cooling channels comprise

straight cooling channels (SCCs) produced with drilling machines. By suitably arranging cooling channels, the molding cycle time can be reduced and defects such as short shots, residual stress, shrinkage, and warpage prevented (Park and Dang, 2012; Marques et al., 2015; Kuo et al., 2020; Wang et al., 2011; Tan et al., 2020; Wang et al., 2015). In practice, cooling channels must be designed to avoid interference with the ejection system and with consideration of the processing intensity. Improperly designed cooling channels do not provide even cooling, resulting in defects. Thus, an adequate cooling channel design is critical for minimizing the molding cycle time and yielding high-quality parts.

Cooling occurs throughout the injection molding cycle. After melt enters the mold, the cooling channel fluid cools the mold until the melt hardens and is removed. Cooling channels are expected to provide rapid and even cooling, but conventional SCC designs are due to limitations in channel processing methods (Fig. 1(a) and are thus unable to provide an optimal cooling effect. Technological advancements have enabled the production of conformal cooling channels (CCCs) with three-dimensional (3D) printing (Fig. 1b). Molds with such channels have reduced molding cycle time, improved production efficiency, and improved product quality. Scholars have asserted that such cooling channels are the most promising method for reducing molding cycle time and have proposed numerous methods for creating CCCs (J. Meckley & R. Edwards, 2009). However, these studies typically use simulations to verify these methods because of the high costs of producing 3D-printed molds. Nevertheless, relevant studies have been continued because of the potential of CCCs for reducing the molding cycle time and increasing product quality.

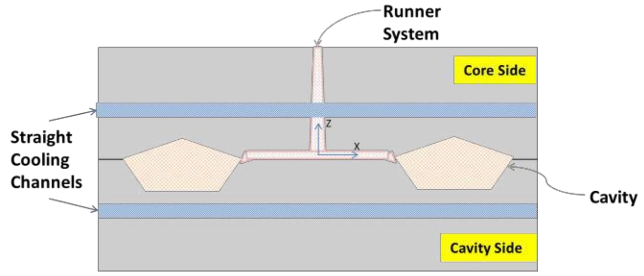

(a)

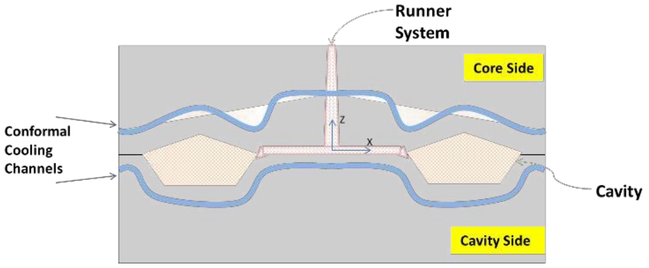

(b)

**Fig. 1.** Comparison of (a) SCC and (b) CCC configurations

Cooling channel-based cooling systems are crucial to injection molding. During data collection, this study discovered that all studies on CCCs have adopted two assumptions in model design: the use of (1) a hot runner system and (2) a one-mold-one-cavity design. These assumptions substantially simplify the research. A runner system delivers pressure and melt to the mold and has a smooth surface to minimize energy and pressure losses. Hot runner systems include a heater, and therefore eliminate waste that remains in the runner in a cold runner system. If the melt in the runner system freezes before the cavity melt does, problems such as short shots and sink marks may frequently occur. Therefore, previous CCC studies have assumed the use of hot runner systems to ensure that the cooling time of the runner system is longer than that of the cavity; this enables them to focus on minimizing part cooling time and neglect short shot and sink mark defects. The one-mold-one-cavity assumption is that cooling channels only cool a single product. However, most molds are designed with multiple cavities (Fig. 1); the cooling fluid removes heat from both the core side (that near the runner system) and the cavity side of the mold. The quality of the products produced on the two mold sides may differ. These two assumptions may not apply to all commercial systems; hence, a design method for honeycomb CCCs for cold runner systems and multiple cavities is proposed in this study. Specifically, an algorithm was developed to automatically design CCCs for such systems. This algorithm can be used to reduce the cooling time, improve product quality, and ensure that the system temperature is relatively homogenous in practical situations.

## 2. Literature review

Many products with curved surfaces are produced in injection molding, and CCCs are the most effective methods for reducing the cooling time of such products. Numerous studies have explored CCCs; however, few have examined the automatic design of such channels or the application of CCCs in cold runner systems or molds with multiple cavities. In this study, a literature review was first performed to identify research on CCC design stages and to systematically compile the CCC design method. The review revealed that most designs used to offset, feature, and hotspot adjustment methods. In addition, this study noted that few studies have investigated automated CCC design. In the conclusion section, a summary of previous research is presented to highlight the novel contributions of this study to CCC development processes.

### 2.1. Design Stages of CCCs

The CCC design process is complex. Studies have proposed various methods for designing CCCs; however, discrepancies exist among these methods. Some design methods are based on experience; however, experience-based methods are not user-friendly. Li et al. (2005) proposed a novel design method involving three stages: preliminary design, layout design, and detail design. Table 1 summarizes each stage of the method. Our literature review also indicated that most subsequent studies adopted these stages to examine CCC design. Therefore, previous studies were analyzed based on these three stages.

Preliminary design is the foundation of channel design. It involves two main tasks: cavity shaping and cooling element addition. The cavity shape determines the shape of the produced part, and cooling elements are configured under the cavity shape. Cooling elements may be adjusted based on the offset of the cavity shape to ensure that the distance between cooling elements and the cavity is constant, (Au and Yu, 2006; Park and Pham, 2009; Wang et al., 2011; Goktas et al.,2016). Other adjustment methods based on cavity offsets involve modularized design, in which the space between the center of a cooling element and the mold cavity is occupied by solid steel, and cooling channels compose the remaining space. Such methods yield conformal cooling cavities and may enable skipping the layout design stage, thereby simplifying the cooling channel design stages (Au and Yu, 2007; Brooks and Brigdam, 2016; Kanbut et al., 2019; Oh et al., 2022). Cooling element addition is the other key task of preliminary design. A cooling element might be a node or line. Most studies on cooling element design have focused on automated cooling channel design (Li et al., 2005; Wang et al., 2011; Au et al., 2011; Au and Yu, 2014). This study asserted that automated design requires all cooling elements of a cooling channel system to be comprehensively defined to ensure meeting the system's requirements. Defining a cooling element is equivalent to defining a cooling target.

**Table 1.** CCC design stages

| Stage | Main Function | Description |
|---|---|---|
| **Preliminary Design** | *Cavity Shape<br>*Cooling Element<br>*Boundary Condition | Preliminary design involves two primary tasks: cavity shaping and cooling element addition. The configuration of boundary conditions, including thickness and temperature fields, must be carefully analyzed. |
| **Layout Design** | *Connect Cooling Element<br>*Connect Sub Cooling Channels | In layout design, the designer ensures that the cooling elements are adequately connected to form a water channel. Neighboring subchannels must connect properly to form complete channels. |
| **Detail Design** | *Channel Diameter<br>*Cross-Sectional Shape<br>*Channel Features | A complete channel layout might be presented as a line structure, which requires further design of structural details. The objective of detail design is to concretize a layout by configuring characteristics such as channel diameter, cross-sectional shapes, and channel features. |

By contrast with manual design, which relies on experience or intuition, automated design requires comprehensive definitions. Because preliminary design is the first stage of cooling channel design, this study focused on this design stage.

However, layout design and detail design must also be clearly defined to achieve automated cooling channel design. Therefore, these two stages are briefly introduced in this section. The primary goal of the layout design is to form subchannels to connect the cooling elements established in the preliminary design. These subchannels are subsequently connected to form a complete cooling channel (Li et al.,2005; Au et al., 2011; Hu et al., 2016; Choi et al., 2014). Layout design might only yield a simple line structure; the details of this structure must be determined in the detail design stage. Specifically, detail design focus on concretizing a line structure by determining its structural characteristics, including channel diameter, cross-sectional shapes, and channel features (Au and Yu, 2006; Saifullah and Masood, 2007; Altaf et al., 2011). This study only focused on the preliminary design stage and did not analyze the layout and detail design stages in depth; standard methods were used for these two stages to enable the final analysis.

## 2.2. Adjustment of CCCs

Of the three design stages introduced in Section 2.1, a preliminary design has garnered the most attention from scholars because the configuration of boundary conditions and design elements are crucial to cooling channel design.

Cooling element selection is the key process in CCC research because it reflects the principles of channel design. To further explore these principles, the design process was not only divided into three stages, but cooling channels were also categorized into those configured using the offset, feature, or hotspot adjustment methods. Offset is the shifting of a cooling element based on its distance from the cavity contour; this distance is fixed to ensure that the distance between the center line of the element and the cavity is constant. Offset distance configuration is the most frequently studied adjustment method in CCC design research. Feature adjustment designs are based on cavity features and are primarily based on designer intuition. The method might involve stacking specific cooling channels, such as bubbler, baffle, or helix channels, and is mainly used to address specific problems, such as part shrinkage. In the hotspot adjustment method, a channel design is configured based on the temperature distribution after filling. The distance from each cooling element center to the cavity can be constant or varied. This method must be used in combination with mold flow analysis or physical measurements and thus is less frequently used for CCC design. Studies on the hotspot adjustment method also appeared later than research on the other two methods. The goal of this method is to minimize the overall temperature heterogeneity of the melt. Table 2 summarizes the differences between the offset, feature, and hotspot adjustment methods.

**Table 2.** Differences between the configuration methods of cooling channels**Channel–cavity distance**

| | Channel–cavity distance | Automation | Auxiliary method | Naming |
|---|---|---|---|---|
| **Offset** | Constant | Easy | NA | CVD (Y. Wang et al., 2011), PCCC (K. Altaf et al., 2011) |
| **Feature** | Constant/varied | Difficult | Feature definition | MGSS (S. Z. A. Rahim et al., 2016) FBA (C. L. Li, 2001)<br>C-Space (C.G. Li & C.L. Li, 2008) CCCAB (H. S. Park & X. P. Dang, 2010), Helix (S. Han et al., 2020) |
| **Hotspot** | Constant/varied | Easy | Analysis of actual temperature | U-Shape MGCCC (X. P. Dang & H. S. Park, 2011) ADE (M. Frings et al., 2017), Non-Equidistant (Y. P. Luh et al., 2019)<br>Thermal-Fluid Topology (T. Wu & A. Tovar, 2018) TCMDM (A. Torres-Alba et al., 2020) |

## 2.3. Automation Design of CCCs

Sections 2.1 and 2.2 reveal that various CCC design research directions exist, and some scholars have investigated automated CCC design. However, automated CCC design is challenging because cooling channel targets and frameworks must be clearly defined and because a thorough understanding of programming and mathematics is required. Table 3 lists relevant studies on automated CCC design. In the table, PD, LD, and DD denote preliminary design, layout design, and detail design, respectively; 1 V 1 denotes the one-mold-one-cavity assumption; and 1 V M denotes one-mold-multiple-cavities.

None of the identified studies on automated CCC design over the past decade investigated cold runner systems or molds with multiple cavities. Categorizing these studies by their design stages and methods revealed that few studies,

whether automated or manual, have focused on the detailed design stage. This could be because this stage involves a few researchable variables, such as cross-sectional areas, cross-sectional shapes, and inner-wall texture. Most studies have used offset and feature adjustment methods to configure CCCs; few have used the hotspot adjustment method. This was attributable to the less-intuitive nature of the hotspot adjustment method and its requirement of mold flow analysis software or physical measurements for adjusting the channel distance. Accordingly, subsequent studies should explore the detailed design stage, hotspot adjustment method, and the use of cold runner systems and molds with multiple cavities to highlight new research directions for automated CCC design.

**Table 3.** Methods of automatic CCC design

| *Author/Year* | *Method* | *Design Stage* | *Building Method* | *Cold Runner* | *Cavity Number* |
|---|---|---|---|---|---|
| *C. L. Li, 2001* | Feature-Based Approach | PD/LD | Offset | N | 1V1 |
| *C. L. Li et al.,2005* | Graph Traversal Algorithm | LD | Feature | N | 1V1 |
| *K. M. Au & K. M. Yu, 2007* | Scaffolding Architecture | PD | Offset | N | 1V1 |
| *C.G. Li & C.L. Li, 2008* | The Configuration Space Method | LD | Feature | N | 1V1 |
| *H. S. Park & N. H. Pham, 2009* | Zigzag/ Parallel/ Spiral Type | LD | Hotspot | N | 1V1 |
| *H. S. Park & X. P. Dang, 2010* | Array of Baffles | DD | Feature | N | 1V1 |
| *K. M. Au & K. M. Yu, 2011* | Multi-Connected Porous Passageway | PD | Offset | N | 1V1 |
| *K. M. Au et al., 2011* | Visibility-Based Conformal Cooling Channel | PD/LD | Offset | N | 1V1 |
| *Y. Wang et al., 2011* | Centroidal Voronoi Diagram | PD | Offset | N | 1V1 |
| *J. H. Choi et al., 2014* | Centroidal Voronoi Diagram +Branching Law | LD | Feature | N | 1V1 |
| *K. M. Au & K. M. Yu, 2014* | Variable Distance Conformal Cooling Channel | *PD* | Feature | N | 1V1 |
| *T. Wu et al., 2015* | Multi-Scale Thermo-Mechanical Topology Optimization Algorithm | PD | Offset | N | 1V1 |
| *Y. Wang et al., 2015* | Spiral and Conformal Cooling Channels | PD | Offset | N | 1V1 |
| *M. Goktas et al., 2016* | Spiral-Formed Canal Paths | PD | Offset | N | 1V1 |
| *S. A. Jahan, et al., 2016* | Conformal Cooling Cavities | PD | Offset | N | 1V1 |
| *P. Hu et al., 2016* | Longitudinal/ Transversal/ Parallel/ Serpentine CCC | LD | Offset | N | 1V1 |
| *D. Homar & F. Pušavec, 2016* | Optimized Manufacturing Operation Sequence Algorithm | LD | Feature | N | 1V1 |
| *Z. Li, et al., 2017* | Boundary Element Method + Topology Optimization | LD | Offset | N | 1V1 |
| *Y. M. Zhang et al., 2017* | Conformal Loops Based on Geometric + Centre Lines in Spiral Shape | PD | Offset | N | 1V1 |
| *J. M. Mercado-Colmenero et al., 2018* | Baffles Location Via the Genetic Algorithm | DD | Feature | N | 1V1 |
| *Y. P. Luh et al., 2019* | Non-Equidistant Conformal Cooling Channels | PD/LD | Hotspot | N | 1V1 |
| *J. M. Mercado-Colmenero et al., 2019* | Lattice Element Design + Expert Algorithms | PD | Feature | N | 1V1 |
| *A. Torres-Alba et al., 2020* | Temperature Clusters and Multidimensional Discrete Models | PD | Hotspot | N | 1V1 |
| *J. M. Mercado-Colmenero et al., 2021* | Based on the Use of Complex Geometries and Optimization of Temperature Profiles | PD | Feature | N | 1V1 |
| *A. Torres-Alba et al., 2021* | Triple Hook-Shaped Conformal Cooling Channels | PD | Feature | N | 1V1 |

**Note:**
***Preliminary Design=PD , Layout Design=LD , Detail Design=DD**
***One Mold one Cavity = 1 V 1, One Mold with multiple Cavity = 1 V M**

## 2.4. Summary

A literature review of CCC design studies was conducted to demonstrate the novelty of the proposed automated design method for honeycomb CCCs. Li et al. (2005) first proposed the three-stage concept of preliminary, layout, and detail design. The proposed design stages can serve as the standardized process for designing CCCs and defining essential design elements and were thus adopted in the proposed automatic design method of this study. CCC adjustment methods are divided into offset-based, feature-based, and hotspot-based approaches. Studies have only compared various types of cooling channels (i.e., CCCs and SCCs); they have not investigated the use of different adjustment methods for configuring the same CCC design. This research gap is addressed in this study. In the proposed design method, offset, feature, and hotspot adjustment methods can be combined to configure the distance between the cooling elements and mold cavities. Accordingly, the efficiency of the three methods can be compared to determine the optimal method for automated honeycomb CCC design. None of the 25 studies on automatic CCC design listed in Table 3 have investigated cold runner systems or molds with multiple cavities. Therefore, another contribution of this study is to address this research gap. In sum, the contributions of this study are as follows:

(a) Use the three major design stages to clarify the CCC design process and verify the viability of this process.
(b) Develop an automated honeycomb CCC design method and compare the offset, feature, and hotspot adjustment methods.
(c) Investigate automated CCC design for cold runner systems and address the problem of short shots and the requirement of using energy (heat and pressure) to deliver melt to the flow end.
(d) Consider molds with multiple cavities to reduce the temperature differences between the cavities, reduce product defects caused by these temperature differences, and ensure that the proposed design method is in line with practical needs.

## 3. Methodology

The proposed automated design method was developed to reduce product defects and reduce the molding cycle time. Honeycomb CCCs are regular hexagon cooling channels that are closely connected on an *XY* plane; the resulting structure resembles a honeycomb (Fig. 2). The *z* distance between the six nodes of each hexagon and the mold cavity differs based on the adopted adjustment method (Fig. 1b). The use of regular hexagons as cooling elements in this study was inspired by Xu et al. (2004), who adjusted the channel–cavity distance based on the spacing between channels. Because the distance between each node of a regular hexagon and its center and that between two neighboring nodes is constant, the use of regular hexagons and nodes to form cooling elements was assumed to facilitate maintaining a homogenous temperature distribution across the part surface. Moreover, because the distance between each node of a regular hexagon and its center is constant, the sprue of a cold runner system can be installed at the center of the cooling channel arrangement to ensure that it cools evenly and to prevent the tangency or overlaying of the sprue and nodes. The automated design method for honeycomb CCCs was developed by employing various adjustment methods and examining their effects on the molding cycle time and part quality in a system with a cold runner and multiple-cavity mold.

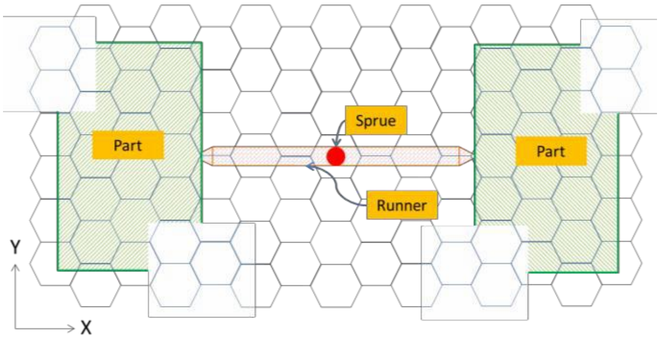


**Fig. 2.** Illustration of honeycomb CCCs

### 3.1. Building Procedure

The water channels in honeycomb CCC are equidistant. Automated CCC design requires establishing a standardized design process; the three design stages introduced in Section 2.1 were adopted (Fig. 3). Specifically, the preliminary design stage was divided into obtaining cavity information, adding the cooling elements, and adjusting the cooling elements. The layout design layer was divided into connecting the cooling elements and connecting the sub-cooling channels. The detail design stage only involves body giving. A detailed flow chart of the design stages is presented in Fig. 4. Standard methods of interconnecting the hexagonal cooling elements and determining the channel diameter were used in the layout and detail design stages. Finally, the three adjustment methods were used to configure the channel arrangement to optimize the automated design method for applications with cold runner systems and molds with multiple cavities.

A detailed flow chart of the preliminary design stage is presented in Fig. 4. By Fig. 3, this stage is divided into obtaining cavity information, cooling element addition, and cooling element adjustment. In obtaining cavity information, the position of the sprue is determined and used as the center of the entire channel structure to divide the individual cooling elements (Fig. 2). In cooling element addition, hexagonal cooling elements on the xy plane are generated by using the sprue as the center. This step involves defining the cooling element radius, adding the honeycomb elements, rotating the elements, and expanding the elements. Finally, in cooling element adjustment, the runner and part are identified and the three adjustment methods are implemented. Overall, obtaining cavity information is a simple process; the other steps require using algorithms to obtain an accurate honeycomb CCC structure arrangement. Sections 3.2 and 3.3 describe these two steps in detail.

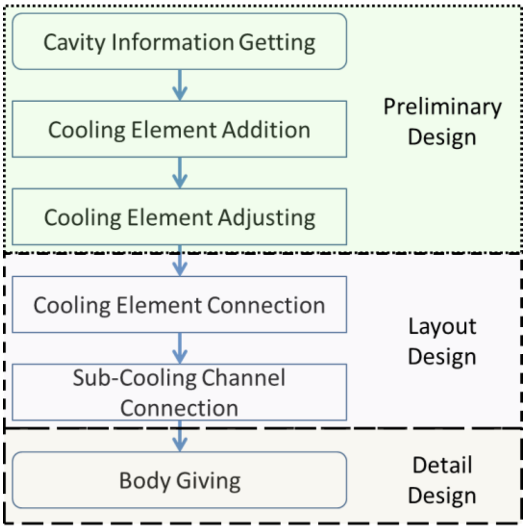


**Fig. 3.** Flowchart of a cooling channel design process

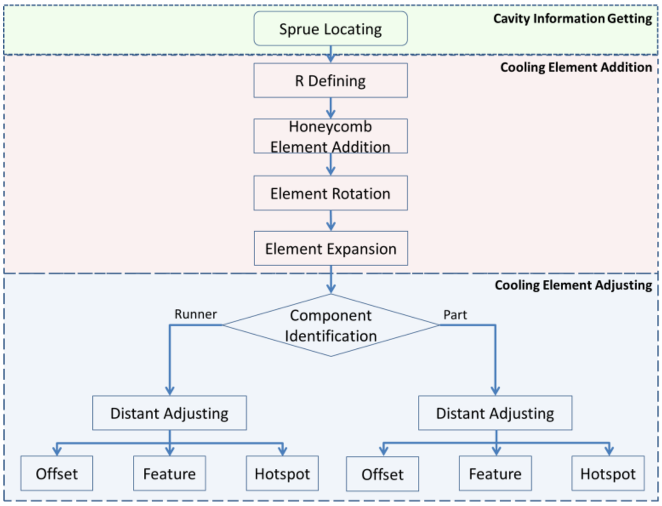


**Fig. 4.** Flowchart of the preliminary design stage

## 3.2. Cooling Element Addition

The arrangement of regular hexagonal cooling elements ensures equal distances between the hexagon center and each node and between neighboring nodes. The hexagonal shape simplifies the calculation of the mutual effect between individual water channels. If a regular hexagon is surrounded by a circle with each corner (node) touching the circle, the distance between the center and each node and each side of the hexagon is equal to the radius *R* of the circle (Fig. 5). The center is defined as the position of the sprue, which is located at $[x_0, y_0]$.

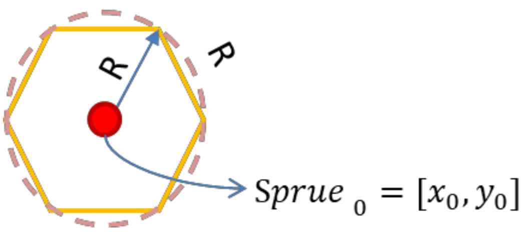


**Fig. 5.** Hexagonal cooling element

*R* affects the arrangement of cooling elements. Factors affecting *R* include the channel diameter and cavity size. The channel diameter of typical SCCs is 8–12 mm. CCCs created with 3D printing must be at least 5 mm apart from each other to prevent the collapse of the channels. The relationship between two neighboring nodes is presented in Fig. 6: The vertical distance between Nodes H3 and H4 is $(R\sqrt{3})/2$. The channel diameter is *D*, and the distance between the center lines of two parallel channels is 2*D*. Accordingly, Equation (1) can be used to determine *R* as follows.

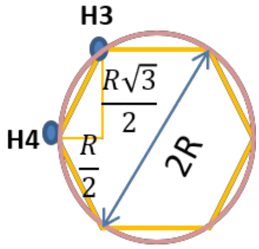


**Fig. 6.** Relationship between two neighboring nodes of a honeycomb cooling element

$$R \geq \frac{2D}{\sqrt{3}}; D = 8 \backsim 12 \quad (1)$$

After determining *R* for the first cooling element, element rotation must be performed for the feature and hotspot adjustment methods; the offset adjustment method does not require this process. Element rotation ensures that specific elements can be positioned in the area of interest, such as areas where specific features are located, areas with adequate thickness, or the area with the highest temperature. Although the goal of element rotation varies, the same rotation method is applied. The sprue location is selected as the coordinate origin, and the nodes of each cooling element are 60° apart. If the rotation angle is $\theta_h$ and the original node positions are H1 = 0°, H2 = 60°…, then Equation (2) can be used to determine the position of each node after rotation following Fig. 7.

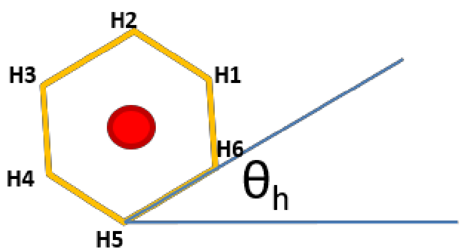


**Fig. 7.** Rotation of a cooling element

$$\mathrm{Hi} = \left[x_0 + R\cos\left(60^{\circ}(i-1) + \theta_h\right), y_0 + R\sin\left(60^{\circ}(i-1) + \theta_h\right)\right] \quad ; i = 1, \ldots, 6 \quad (2)$$

After establishing the first honeycomb cooling element by using the sprue as the center, the other elements are added through radial expansion with the first element as the radial center (Fig. 8). The coordinate of the first element is equal to that of the sprue$_s$, or $[x_s, y_s]$. Six new centers 60° apart are added through radial expansion from the first element.

Equation (3) presents the radial expansion formula. This equation is used in combination with Equation (2) to derive the position of each node of the newly added elements. Each new element then serves as a radial center for adding more elements until the model cavity is filled.

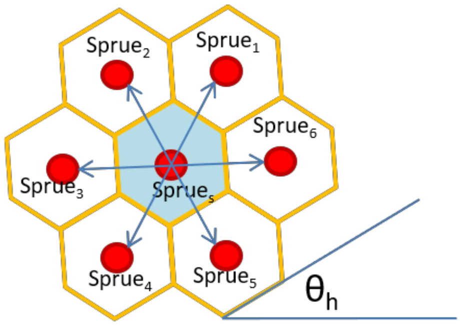


**Fig. 8.** Expansion of cooling elements

$$\mathrm{Sprue}_i = \left[x_s + 2R\cos\left(60^\circ(i-1) + 30^\circ + \theta_h\right), y_s + 2R\sin\left(60^\circ(i-1) + 30^\circ + \theta_h\right)\right] \quad ; i = 1,..,6 \tag{3}$$

## 3.3. Cooling Element Adjustment

This step involves adjusting the distance between each element node and the mold cavity. After completing the arrangement of all cooling elements on the *xy* plane of the cavity, relevant components for adjusting the *z*-direction of each node are identified. The runner must not freeze before the part does; otherwise, the provision of melt and pressure will be insufficient. Therefore, component identification is performed to adjust the *z*-direction of the cooling channels.

Distance calculation was a crucial step in the preliminary design stage of this study. After determining the position of each element node and identifying all relevant components, three adjustment methods were used to configure the distance between each cooling element and the cavity surface. *White Paper Conformal Cooling*, published by Hall (2015), states that, in CCCs, the distance between a mold cavity and the center line of a cooling channel must be at least 1.5 times the channel diameter; this distance is also used as the offset distance in the offset adjustment method. In this study, the channel diameter was denoted as *D*; thus, the offset distance was adjusted using Equation (4). To ensure that the runner does not freeze before the part does, Equation (5) was introduced to offset the channel above the runner by an additional distance of *D*.

$$L_{m,o-p} = 1.5D \tag{4}$$

$$L_{m,o-r} = 2.5D \tag{5}$$

Fig. 9 illustrates the thermal equilibrium and transfer of a mold in accordance with Xu et al. (2004). $Q_p$ denotes the heat of the part to be produced and is the input value. $Q_m$ and $Q_c$ denote the heat removed by the mold and cooling channel, respectively, and are the output values; hence, $Q_p = Q_m + Q_c$.

Because the heat loss on the outer mold surface is less than 5% of the total heat loss during injection molding, Park and Kwon (1998) asserted that this surface is thermally insulative. Accordingly, the aforesaid equation can be simplified to $Q_p = Q_c$. Equations (6) and (7) are used to calculate $Q_p$ and $Q_c$, respectively; please refer to the Nomenclature table for the definition of each symbol.

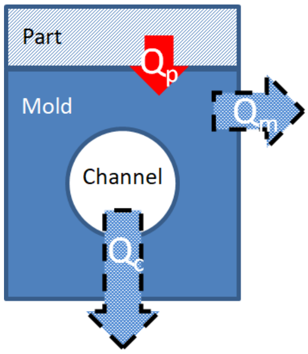


**Fig. 9.** Thermal equilibrium of a mold

$$Q_p = \frac{\rho_p C_p t_p W_c (T_{melt} - T_{eject})}{t_{cycle}} dt \tag{6}$$

$$Q_c = \frac{h\pi D (T_m(t) - T_c) k_m W_c}{2k_m W_c + h\pi D L_m} dt \tag{7}$$

After rearranging the two equations, the thickness feature was used as the basis for distance adjustment. Because $T_m(t) = T_{melt}$ and $L_{m,o-p} = 1.5D$, Equation (8) can be expressed as follows. In this equation, only the thickness variable $t_p$ varies between different node positions; the other variables can be determined with a reference table or as preset values. Because the runner must not freeze before the part does, a time constant $t_r$ is added to the cycle time [Equation (9)], which is further explored in the subsequent analysis.

$$L_{m,f-p} = \frac{2t_{cycle} k_m (T_{melt} - T_c)}{\rho_p C_p t_p W_c (T_{melt} - T_{eject})} - \frac{2k_m W_c}{h\pi D} + \frac{3D}{2} \tag{8}$$

$$L_{m,f-r} = \frac{2k_m (t_{cycle} + t_r)(T_{melt} - T_c)}{\rho_p C_p t_p W_c (T_{melt} - T_{eject})} - \frac{2k_m W_c}{h\pi D} + \frac{3D}{2} \tag{9}$$

Equations (9) and (10) were obtained by rearranging Equations (6) and (7) and by referencing the hotspot adjustment equation used by Luh et al. (2019). $T_m(t)$ denotes the node temperature, which is determined through a temperature distribution map obtained from mold flow analysis. The time constant $t_r$ is also added to Equation (10) to ensure that the runner does not freeze before the part does.

$$L_{m,h-p} = \frac{k_m [T_m(t) - T_c] t_{cycle}}{\rho_p C_p L_p (T_{melt} - T_{eject})} - \frac{2k_m W_c}{h\pi D} + \frac{3D}{2} \tag{10}$$

$$L_{m,h-r} = \frac{k_m [T_m(t) - T_c](t_{cycle} + t_r)}{\rho_p C_p L_p (T_{melt} - T_{eject})} - \frac{2k_m W_c}{h\pi D} + \frac{3D}{2} \tag{11}$$

The proposed automated design method is compatible with the offset, feature, and hotspot adjustment methods for configuring the distance between each cooling element node and the mold cavities. In the design method, a mold cavity is divided into two regions, the part, and the runner, and the time constant $t_r$ ensures that the runner does not freeze before the part does. To verify the effectiveness of the proposed design method and compare the characteristics of the three adjustment methods, we performed a case study by using the model adopted by Luh (in production). The goal was to confirm whether the honeycomb CCCs arranged using the proposed method can reduce the cooling time, improve part quality, and maintain an even temperature distribution.

## 4. Result and Discussion

In this case study, the differences between the three honeycomb CCC adjustment methods were compared to verify that the cooling channels arranged using the proposed design method are more effective for reducing the cooling time, improving part quality, and maintaining an even temperature distribution than conventional SCCs are. The model adopted by Luh (in production) also included a cold runner system and a mold with two cavities. Fig. 10 presents the model; it has two sides, one side is flat and the other has height differences. The plastic parts had a length, width, and height of 240, 60, and 21 mm, respectively. The thickness distribution of the aforementioned parts is illustrated in Fig. 10, with the thickness ranging from 1.85 to 21 mm. The Moldflow software was used to simulate and assess the effectiveness of the arranged honeycomb CCC structure. To ensure the objectivity of this study, its results were compared with those obtained from an SCC model and those obtained by Luh (in production) in terms of temperature distribution, volumetric shrinkage, and warpage. In the Moldflow software, the tetrahedral elements are used on the whole model, including the part, runner system, CCC, and mold. The material of the part and runner system is PP, while the coolant is water and the mold is a 20 tool steel. All the material property in the Moldflow software is shown in Table 4.

Four analysis models and a reference study were compared. The four models were (a) an SCC model, (b) a honeycomb CCC model configured using the offset adjustment method (denoted OC), (c) a honeycomb CCC model configured using the feature adjustment method (FC), and (d) a honeycomb CCC model configured using the hotspot adjustment method (HC) (Fig. 11) The model of Luh (in production) was also used for some comparisons.

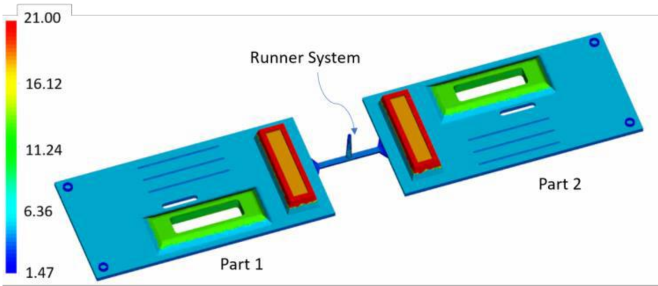


**Fig. 10.** Thickness distribution of the model

**Table 4.** Material Thermal Property

| Material | Specific Heat (J/kg-C) | Thermal Conductivity (W/m-C) | Density (g/cm3) |
|---|---|---|---|
| PP | 2887 | 0.1752 | 0.8942 |
| Water | 4180 | 0.643 | 0.988 |
| P-20 Tool Steel | 460 | 29 | 7.8 |

The three honeycomb CCC models were constructed using the proposed design method, and their honeycomb structures were observed on the *XY* plane. However, because the models were configured with different adjustment methods, considerable distance differences were observed in the *xz*-plane; the differences in the distance between the cooling channels and runner systems were particularly large.

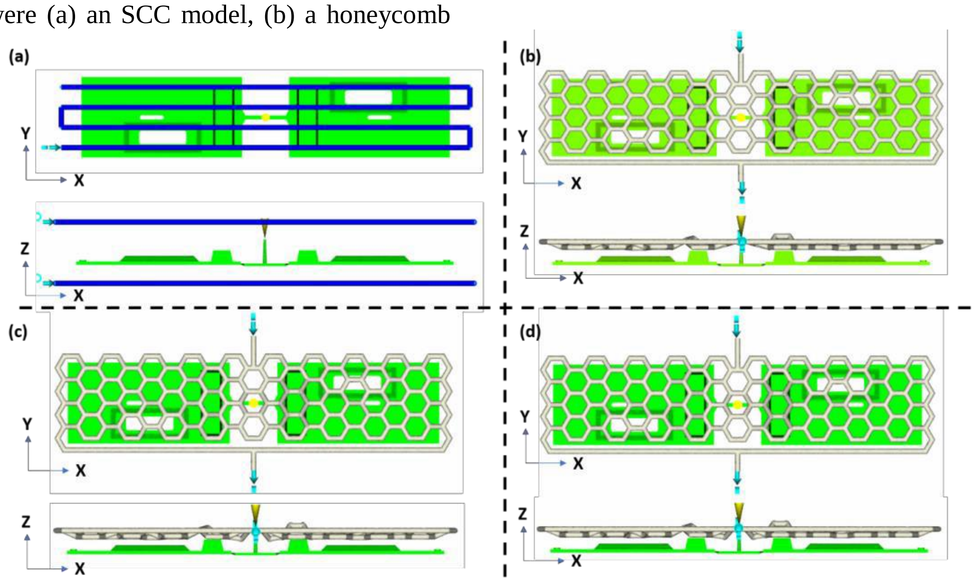


**Fig. 11.** Analysis of models (a) SCC, (b) OC, (c) FC, (d) HC

### 4.1. Temperature Distribution

Cooling channels in a mold cooling system should rapidly and uniformly reduce the temperature of the cavity and the plastic to ensure even part shrinkage and high part quality. Temperature simulation results obtained from Moldflow were used to determine the temperature distribution after the cooling process and before the ejection process. Fig. 12 presents the temperature distributions of the four models; the temperature range is 29°C–65°C. The results revealed that the SCC temperature was greater than that of OC, FC, or HC. Table 5 presents a comparison of the temperature at ten points in Part 1, ten points in Part 2, and four points in the runner; these measurement points were identical to those adopted by Luh (in production) to facilitate the comparison. The results are summarized in row (e) of Table 5.

**Table 5.** Temperature Distribution

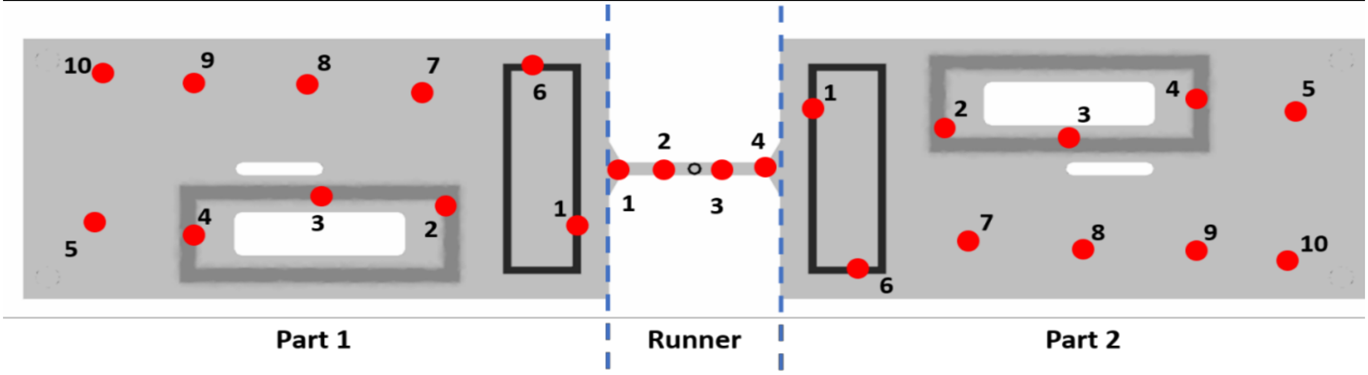


| | Unit: °C | P1-1 | P1-2 | P1-3 | P1-4 | P1-5 | P1-6 | P1-7 | P1-8 | P1-9 | P1-10 | Ave. | Diff. |
|---|---|---|---|---|---|---|---|---|---|---|---|---|---|
| *Part 1* | (SCC) | 46.84 | 57.78 | 50.67 | 49.78 | 51.07 | 51.58 | 55.93 | 53.15 | 50.40 | 46.65 | 51.39 | 11.13 |
| | (OC) | 33.52 | 41.67 | 37.57 | 37.36 | 39.56 | 38.61 | 39.74 | 38.61 | 38.37 | 37.19 | 38.22 | 8.15 |
| | (FC) | 33.02 | 41.12 | 37.34 | 36.97 | 39.14 | 38.16 | 39.26 | 38.19 | 37.89 | 36.91 | 37.80 | 8.10 |
| | (HC) | 33.09 | 41.34 | 37.49 | 37.26 | 39.43 | 38.40 | 39.56 | 38.43 | 38.07 | 37.06 | 38.01 | 8.25 |
| | (Luh) | 34.08 | 46.97 | 41.81 | 39.61 | 43.39 | 33.29 | 44.91 | 44.38 | 43.83 | 42.85 | 41.51 | 13.68 |
| | **Unit: °C** | **P2-1** | **P2-2** | **P2-3** | **P2-4** | **P2-5** | **P2-6** | **P2-7** | **P2-8** | **P2-9** | **P2-10** | **Ave.** | **Diff.** |
| *Part 2* | (SCC) | 47.82 | 58.45 | 50.90 | 50.99 | 50.77 | 51.63 | 56.89 | 52.94 | 49.38 | 46.65 | 51.64 | 11.80 |
| | (b) | 33.34 | 41.36 | 37.18 | 37.10 | 39.40 | 40.62 | 40.20 | 39.35 | 38.72 | 38.27 | 38.55 | 8.02 |
| | (OC) | 32.83 | 40.85 | 36.92 | 36.74 | 39.05 | 40.29 | 39.70 | 39.00 | 38.50 | 38.05 | 38.19 | 8.02 |
| | (FC) | 33.08 | 41.17 | 37.09 | 36.95 | 39.26 | 40.47 | 39.96 | 39.21 | 38.68 | 38.23 | 38.41 | 8.09 |
| | (HC) | 34.08 | 46.97 | 41.81 | 39.61 | 43.39 | 33.29 | 44.91 | 44.38 | 43.83 | 42.85 | 41.51 | 13.68 |
| | **Unit: °C** | **R1** | **R2** | **R3** | **R4** | | | | | | | **Ave.** | **Diff.** |
| *Runner* | (SCC) | | 46.16 | | 39.90 | 40.20 | | 46.33 | | | 43.15 | | 6.43 |
| | (OC) | 37.35 | 32.26 | 32.47 | 37.73 | | | | | | | 34.95 | 5.47 |
| | (FC) | | 36.45 | | 31.68 | 31.90 | | 36.99 | | | 34.26 | | 5.31 |
| | (HC) | 36.63 | 31.78 | 31.99 | 37.15 | | | | | | | 34.39 | 5.37 |

Table 5 lists the temperature at each measurement point. A comparison of the 10 points in Part 1 revealed that SCC had the highest mean temperature, whereas FC had the lowest temperature. Regardless of the adjustment methods adopted, the temperature of all honeycomb CCC models was lower than those of SCC and Luh's models. A similar trend was observed in Part 2. In addition to examining the mean temperature of the measurement points, their temperature differences were analyzed. The results revealed that temperature differences of the three honeycomb CCC models were approximately 8°C, whereas those of the SCC and Luh models were >10°C (Table 5). This result verifies that the honeycomb CCCs arranged using the proposed design method could effectively reduce the mean temperature and temperature difference in mold cavities. The results also confirmed that the mean temperature near the runner system was lower in the honeycomb CCC models than in the SCC model. Finally, this study examined the time to produce the frozen layer and observed that the runner system began to freeze at 7.5 s in both the CCC and SCC models. Thus, the honeycomb CCCs did not causepremature freezing of the runner system.

## 4.2. Volumetric Shrinkage

Volumetric shrinkage refers to the difference in the intended and actual volumes of a produced part. A shrinkage value close to 0 indicates that the actual volume is nearly identical to the intended volume. Uneven shrinkage can create defects on the product surface. Fig. 13 compares the volumetric shrinkage of the four models; it ranged between 1.25% and 15.78%. The differences in the volumetric shrinkage were small. Physical measurements were conducted at the same measurement points used in Table 5, and the results are compiled in Table 6. Luh's model was not used for comparison because Luh (in production) used a different runner system, which could lead to differences in volumetric shrinkage.

Table 6 lists the shrinkage measurement results. The 10 measurement points in Part 1 reveal that the SCC and OC had the highest and lowest levels of shrinkage, respectively. Regardless of the adopted adjustment methods, all honeycomb CCC models had less shrinkage than the SCC model. A similar trend was observed for Part 2. For the SCC model, the shrinkage of Part 1 was lower than that of Part 2. This difference might be attributable to how the cooling fluid arrived at the cavity for Part 1 first before traveling to that of Part 2, causing the temperature of Part 1 to be lower, thus resulting in less shrinkage. By contrast, the cooling fluid inlet of the CCC models was positioned at the center, allowing the fluid to travel to both cavities at the same time; accordingly, Parts 1 and 2 had similar shrinkage. Although the CCC models had less shrinkage than the SCC model, their mean shrinkage still exceeded 10%, which was relatively high. Analysis of the frozen layer revealed that the freezing of the sprue prevented the runner system from providing sufficient pressure and melt to the cavities, causing the resulting parts to shrink considerably. Because the honeycomb CCCs did not cause the sprue to freeze early compared with the reference SCC model, improvements should be made to the runner system itself to ensure that the provision of pressure and melt is sufficient. Overall, the volumetric shrinkage differed between parts in the SCC model but was approximately constant for the CCC models, verifying that the proposed design method is effective for ensuring an even temperature distribution in a mold with two cavities.

**Table 6.** Volumetric shrinkage

| | **Unit:%** | **P1-1** | **P1-2** | **P1-3** | **P1-4** | **P1-5** | **P1-6** | **P1-7** | **P1-8** | **P1-9** | **P1-10** | **Ave.** | **Diff.** |
|---|---|---|---|---|---|---|---|---|---|---|---|---|---|
| **Part 1** | (SCC) | 10.57 | 14.33 | 11.83 | 13.95 | 9.76 | 7.92 | 9.89 | 9.27 | 9.76 | 9.63 | 10.69 | 6.41 |
| | (OC) | 11.14 | 14.09 | 12.03 | 13.84 | 9.41 | 8.59 | 9.27 | 8.69 | 9.23 | 9.36 | 10.57 | 5.50 |
| | (FC) | 11.15 | 14.12 | 12.06 | 13.87 | 9.40 | 8.79 | 9.37 | 8.62 | 9.24 | 9.40 | 10.60 | 5.50 |
| | (HC) | 11.15 | 14.13 | 12.06 | 13.88 | 9.42 | 8.80 | 9.38 | 8.61 | 9.24 | 9.41 | 10.61 | 5.52 |
| | **Unit: ℃** | **P2-1** | **P2-2** | **P2-3** | **P2-4** | **P2-5** | **P2-6** | **P2-7** | **P2-8** | **P2-9** | **P2-10** | **Ave.** | **Diff.** |
| **Part 2** | (SCC) | 11.15 | 14.45 | 11.99 | 13.85 | 9.73 | 11.56 | 9.73 | 9.26 | 9.65 | 9.57 | 11.09 | 5.19 |
| | (OC) | 10.99 | 14.19 | 11.20 | 13.72 | 9.37 | 9.75 | 9.49 | 8.79 | 9.21 | 9.44 | 10.62 | 5.40 |
| | (FC) | 11.14 | 14.21 | 11.86 | 13.78 | 9.42 | 11.52 | 9.47 | 8.69 | 9.06 | 9.31 | 10.85 | 5.52 |
| | (HC) | 11.15 | 14.22 | 11.80 | 13.78 | 9.42 | 11.53 | 9.48 | 8.69 | 9.06 | 9.31 | 10.84 | 5.53 |
| | **Unit: ℃** | **R1** | **R2** | **R3** | **R4** | | | | | | | **Ave.** | **Diff.** |
| **Runner** | (SCC) | 2.29 | 1.88 | 1.87 | 2.46 | | | | | | | 2.13 | 0.59 |
| | (OC) | 2.38 | 2.29 | 2.35 | 2.44 | | | | | | | 2.37 | 0.15 |
| | (FC) | 2.50 | 2.03 | 1.99 | 2.51 | | | | | | | 2.26 | 0.52 |
| | (HC) | 2.50 | 2.09 | 1.99 | 2.52 | | | | | | | 2.28 | 0.53 |

**Table 7.** Warpage

| | **Unit:mm** | **P1-1** | **P1-2** | **P1-3** | **P1-4** | **P1-5** | **P1-6** | **P1-7** | **P1-8** | **P1-9** | **P1-10** | **Ave.** | **Diff.** |
|---|---|---|---|---|---|---|---|---|---|---|---|---|---|
| **Part 1** | (SCC) | -4.23 | -2.53 | -0.36 | 2.30 | 5.19 | -3.98 | -2.42 | -0.10 | 2.65 | 4.81 | 0.13 | 9.43 |
| | (OC) | -2.25 | -1.09 | -0.05 | 1.25 | 2.51 | -2.12 | -1.05 | 0.01 | 1.22 | 1.95 | 0.04 | 4.76 |
| | (FC) | -1.77 | -0.84 | -0.07 | 0.92 | 1.93 | -1.64 | -0.68 | 0.11 | 1.02 | 1.55 | 0.05 | 3.70 |
| | (HC) | -1.95 | -0.93 | -0.07 | 1.07 | 2.19 | -1.85 | -0.83 | 0.04 | 1.10 | 1.73 | 0.05 | 4.14 |
| | **Unit: ℃** | **P2-1** | **P2-2** | **P2-3** | **P2-4** | **P2-5** | **P2-6** | **P2-7** | **P2-8** | **P2-9** | **P2-10** | **Ave.** | **Diff.** |
| **Part 2** | (SCC) | -4.14 | -2.34 | -0.27 | 2.37 | 5.07 | -3.84 | -2.38 | 0.05 | 2.90 | 4.98 | 0.24 | 9.21 |
| | (OC) | -2.17 | -1.07 | -0.07 | 1.20 | 2.45 | -2.10 | -1.01 | 0.02 | 1.29 | 2.07 | 0.06 | 4.62 |
| | (FC) | -1.99 | -1.00 | -0.15 | 0.94 | 2.06 | -1.80 | -0.86 | 0.02 | 1.13 | 1.74 | 0.01 | 4.05 |
| | (HC) | -2.10 | -1.05 | -0.13 | 1.08 | 2.29 | -1.97 | -0.98 | -0.03 | 1.20 | 1.91 | 0.02 | 4.39 |
| | **Unit: ℃** | **R1** | **R2** | **R3** | **R4** | | | | | | | **Ave.** | **Diff.** |
| **Runner** | (SCC) | -4.11 | -4.14 | -4.14 | -4.11 | | | | | | | -4.12 | 0.03 |
| | (OC) | -2.07 | -2.09 | -2.09 | -2.07 | | | | | | | -2.08 | 0.02 |
| | (FC) | -1.59 | -1.67 | -1.74 | -1.76 | | | | | | | -1.69 | 0.17 |
| | (HC) | -1.77 | -1.85 | -1.91 | -1.91 | | | | | | | -1.86 | 0.14 |

### 4.3. Warpage

Warpage refers to the level of deformation of a produced part. A small warpage value (close to 0) indicates minor differences between a produced part and its original design. Fig. 14 presents the warpage value of the four models, which ranged between −4.5 and 7.8 mm. The SCC model had the largest warpage, which was considerably larger than that of the CCC models. Physical measurements were conducted at the same measurement points used in Table 5, and the results are compiled in Table 7.

For the 10 measurement points in Part 1, the SCC and FC models had the largest and smallest warpage, respectively. Regardless of the adopted adjustment methods, the CCC models had less warpage than the SCC model. A similar trend was observed for Part 2. Thus, the proposed design method reduces the occurrence of warpage compared with a conventional design.

## 5. Conclusion

This study proposed an automatic design method for honeycomb CCCs to reduce molding cycle time and improve part quality. This CCC structure comprises a honeycomb-like structure of cooling channels. Studies on CCC design typically assume that molding uses a hot runner system and has a one-mold-one-cavity design. These assumptions effectively simplify pressure exertion and temperature equilibrium, which are key in CCC design. By contrast, the proposed design method applies to cold runner systems and molds with multiple cavities; it is therefore suitable for practical injection molding. Following the cooling channel design stages proposed by Li et al. (2015), this study created a set of standard procedures for automated CCC design. A literature review indicated that three methods of adjusting the distance between cooling channels and cavities in CCC systems are commonly used: offset, feature, and hotspot. However, studies rarely compare the three methods. To address this research gap, the present study redefined the mathematical equations associated with the three methods, applied them in automated honeycomb CCC design, and assessed their effectiveness for avoiding temperature heterogeneity, shrinkage, and warpage. The results verified that honeycomb CCCs could enhance the quality of injection-molded parts.

The efficiency of the proposed method was compared with that of Luh's model using the Moldflow software. The results revealed that, compared with an SCC model, the honeycomb CCC models were more effective at maintaining a homogeneous temperature distribution, reducing shrinkage, and reducing warpage for both parts produced from the same two-cavity mold, thus ensuring consistent part quality. The three adjustment methods achieved similar temperature distributions, temperature differences, volumetric shrinkage, and warpage. Nevertheless, the feature adjustment method was optimal for warpage reduction. The results confirmed that honeycomb CCCs could effectively reduce cavity temperature, improve part quality, and ensure that parts produced from the same multiple-cavity mold maintain consistent quality.

The results of this study can serve as a reference for subsequent research on cooling channels. Honeycomb CCCs can effectively reduce the temperature of mold cavities. Therefore, channels with a large diameter can be installed without increasing the cooling time. However, further research is required to determine the exact channel diameter suitable for CCCs. In addition, the compatibility of different channel types, including three-plate mold, pinpoint gate, and submarine gate channels, with CCCs merits in-depth exploration. This study used a two-cavity mold to verify the effectiveness of honeycomb CCCs in yielding parts with consistent quality. Further research should be performed to confirm whether consistent part quality can be achieved with molds comprising four or more cavities. Additionally, the mold used in this study had uneven thickness. If a mold with even thickness was used, more notable volumetric shrinkage might be observed. Therefore, scholars could explore the effects of different molds on parts with even thickness or curved surfaces. Overall, the results of CCC studies have been limited to applications with hot runner systems and single-cavity molds. The present study addressed this research gap by considering the use of cold runner systems and multiple-cavity molds in accordance with practical injection molding.

## Nomenclature

| | |
|---|---|
| $Q_p$ | Heat from the part |
| $Q_c$ | Heat exchange with coolant |
| $Q_m$ | Heat exchange with environment respectively |
| $\rho_p, \rho_m$ | Density of plastic melt and environment respectively(mold) |
| $C_p, C_m$ | Specific heat of plastic melt and environment respectively(mold) |
| $t_p$ | Thickness of the plastic |
| $L_p$ | Distance of parting line to cavity surface |
| $W_c$ | Pitch distance between central lines of channels |
| $T_{melt}$ | Plastic melt temperature |
| $T_p$ | Plastic ejection temperature at point |
| $T_c$ | Temperature of coolant |
| $T_m, T_a, T_b$ | Temperature of heat point |
| $k_m$ | Thermal conductivity of the mold |
| $h$ | Heat transfer coefficient of coolant |
| $D$ | Diameter of cooling channel |
| $t_{cycle}$ | Injection cycle time |
| R | The Radius of regular hexagon |
| $\theta_h$ | The angle of rotation |
| $Hi$ | The node of regular hexagon |
| $t_r$ | The delay time of cooling |
| $L_{m,o-p}, L_{m,f-p}, L_{m,h-p}$ | The distance between of part and cooling channels |
| $L_{m,o-r}, L_{m,f-r}, L_{m,h-r}$ | The distance between of runner and cooling channels |

## Reference


Altaf, K., Rani, A.M.A., Raghavan, V.R., 2011. Fabrication of Chircular and Profiled Conformal Cooling Channels in Aluminum Filled Epoxy Injection Mould Tools. 2011 National Postgraduate Confernece. Perak, Malaysia.

Au, K.M., Yu, K.M., 2006. Variable Radius Conformal Cooling Channel for Rapid Tool. Material Science Forum, 532, 520-523.

Au, K.M., Yu, K.M., 2007. A Scaffolding Architecture for Conformal Cooling Design in Rapid Plastic Injection Moulding. The Interantional Jpurnal of Advanced Manufacturing Technology, 34, 496-515.

Au, K.M., Yu, K.M., 2011. Modeling of multi-connected porous passageway for mould cooling. Computer-Aided Design, 989-1000.

Au, K.M., Yu, K.M., 2014. Variable Distance Adjustment for Conformal Cooling Channel Design in Rapid Tool. International Journal of Manufacturing Science and Engineering, 136.

Au, K.M., Yu, K.M., Chiu, W.K., 2011. Visiability-based Conformal Cooling Channel Generation for Rapid Tooling. Computed-Aided Design, 43, 356-373.

Brooks, H., Brigdem, K., 2016. Design of Conformal Cooling Layers with Self-Supporting Lattices for Additivel Manufactured Tooling. Additive Manufacturing, 11, 16-22.

Chang, K.H., 2015. Chapter 15 - Product Cost Estimating. In e-Design: Computer-Aided Engineering Design, 787-844, Academic Pr.

Choi, J.H., Kim, J.S., Han, E.S., Park, H.P., Rhee, B.O., 2014. Study on an Optimized Configuration of Conformal Cooling Channel by Brabching Law. Proceeding of the ASME 2014 12th Biennial Conference on Engineering Systems Design and Analysis. Copenhagen, Denmark.

Dang, X.P., Park, H.S., 2011. Design of U-shape Milled Groove Conformal Cooling Channels for Plastic Injection Mold. International journal of precision engineering and manufacturing, 12(1), 73-84.

Frings, M., Behr, M., Elgeti, S., 2017. A Simplified Simulation Model for a HPDC Die with Conformal Cooling Channels. Proceedings of the 20th International ESAFORM Conference on Material Forming.

Goktas, M., Guldas, A., Bayraktar, O., 2016. Cooling of Plastic Injection Moulds Using Conformal Cooling Chanals. 3rd International Conference on Engineering and Natural Science, 2075-2081. Sarajevo, Bosnia.

Hall, M. Krystofik, M., 2015. White Paper Conformal Cooling. Rochester Institute of Technology.

Han, S., Salvatore, F., Bajolet, J., Rech, J., 2020. Abrasive flow machining (AFM) finishing of conformal cooling channels created by selective laser melting (SLM). Precision Engineering, 20-33.

Homar, D., Pušavec, F., 2016. The Development of a Recognition Geometry Algorithm for Hybrid- Subtractive and Additive Manufacturing. Journal of Mechanical Engineering, 151-160.

Hsu, F.H., Wang, K., Huang, C.T., Chang, R Y., 2013. Investigation on conformal cooling system design in injection molding. Advances in Production Engineering & Management(8), 107-115.

Hu, P., He, B., Ying, L., 2016. Numerical Investigation on Cooling Performance of Hot Stamping Tool with Various Channel Designs. Applied Thermal Engoneering, 338-351.

Jahan, A.S., Wu, T., Zhang, Y., Zhang, J., Tovar, A., Elmounayri, H., 2017. Thermo-mechanical design optimization of conformal cooling channels using design of experiments approach. 45th SME North American Manufacturing Research Conference. NAMRC 45, LA, USA.

Jahan, S.A., Wu, T., Zhang, Y., El-Mounayri, H., Tovar, A., Zhang, J., Acheson, D., Nalim, R., Guo, X., Lee, W.H., 2016. Implementation of COnformal Cooling & Topology Optimization in 3D Printed Stainless Steel Porous Structure Injection Molds. Procedia Manufacturing, 901-915.

Kanbur, B.B., Shen, S., Zhou, Y., Duan, F., 2019. Thermal and Mechanical Simulations of the Lattice Structures in the conformal cooling cavities for 3D printed injection molds. Materilas Today: Proceedings, 28, 379-383.

Karthikeyan, S., Jayabal, S., Subramanian, K.S., Chinnakannan, B., 2015. Influence of Cooling Channel Position and Form on Polymer Solidification and Temperature in Injection Molding Die. International Journal for Research in Applied Science & Engineering, 13(98), 447-453.

Kuo, C.C., Jiang, F.Z., Yang, Y.X., Chu, X.S., Wu, Q.J., 2020. Characterization of a direct metal printed injection mold with different conformal cooling channels. The International Journal of Advanced Manufacturing Technology, 1223-1238.

Li, C.G., Li, C.L., 2008. Plastic injection mould cooling system design by the configuration space method. Computer-Aided Design, 334-349.

Li, C.L., 2001. A feature-based approach to injection mould cooling system design. Computer-Aided Design, 1073-1090.

Li, C.L., Li, C.G., Mok, A.C.K., 2005. Automatic layout design of plastic injection mould cooling system. Computer-Aided Design, 37, 645-662.

Li, Z., Wang, X.Y., Gu, J.F., Ruan, S.L., Shen, C.Y., Lyu, Y., Zhon, W., 2017. Topology Optimization for the Design of Conformal Cooling System in Thin-Wall Injection Molding Based on BEM. The International Journal Advanced Manufacturing Technology, 94, 1041-1059.

Luh, Y.P., Chin, C.C., Iao, H.W., (In Production). Automatic design of conformal cooling channel with an asymmetric center. International Journal of Computer Applications in Technology.

Luh, Y.P., Wang, H.L., Iao, H.W., Kuo, T.C., 2019. Using hotspot analysis to establish non-equidistant cooling channels automatically. Journal of the Chinese Institute of Engineers, 690-699.

Marques, S., Souza, F.A., Miranda, R.J., Yadroitsau, I., 2015. Design of conformal cooling for plastic injection moulding by heat transfer simulation. Polímeros, 25(6), 564-574.

Meckley, J., Edwards, R., 2009. A Study on the Design and Effectiveness of Conformal Cooling Channels in Rapid Tooling Inserts. The Technology Interface Journal/Fall, 10, 1-28.

Mercado-Colmenero, J.M., Martin-Doñate, C., Rodriguez-Santiago, M., Moral-Pulido, F., Rubio-Paramio, M.A., 2019. A new conformal cooling lattice design procedure for injection molding applications based on expert algorithms. The International Journal of Advanced Manufacturing Technology, 102, 1719-1746.

Mercado-Colmenero, J.M., Rubio-Paramio, M.A., de J. Marquez-Sevillano, J., Martin-Doñate, C., 2018. A new method for the automated design of cooling systems in injection molds. Computer-Aided Design, 104, 60-86.

Mercado-Colmenero, J.M., Torres-Alba, A., Catalan-Requena, J., Martin-Doñate, C., 2021. A New Conformal Cooling System for Plastic Collimators Based on the Use of Complex Geometries and Optimization of Temperature Profiles. Polymers, 13.

Oh, S.H., Ha, J.W., Park, K., 2022. Adaptive Conformal Cooling of Injection Molds Using Additively Manufactured TPMS Structures. Polymers, 181.

Park, H.S., Dang, X.P., 2010. Optimization of Conformal Cooling Channels with Array of Baffles for Plastic Injection Mold. International Journal of precision engineering manufacturing, 11(6), 879-890.

Park, H.S., Dang, X.P., 2012. Design and Simulation-Base Optimization of Cooling Channels for Plastic Injection Mold. New Technology- Trends, Innovations and Research, 19-44.

Park, H.S., Pham, N.H., 2009. Design of conformal cooling channels for an automotive part. International Journal of Automotive Technology, 10(1), 87-93.

Park, S.J., Kwon, T.H., 1998. Optimal cooling system design for the injection molding process. Polymer Engineering and Science, 38(9).

Rahim, S.Z.A., Sharif, S., Zain, Z.M., Nasir, S.M., Saad, R.M., 2016. Improving the Quality and Productivity of Molded Parts with a New Design of Conformal Cooling Channels for the Injection Molding Process. Advances in Polymer Technology, 35(1).

Saifullah, A.B.M., Masood, S.H., 2007. Optimum Cooling Channels Design and Thermal Analysis of an Injection Moulded Plastic Part Mould. Materials Science Forum, 561-565.

Tan, C., Wang, D., Ma, W.Y., Chen, Y.R,. Chen, S.J., Yang, Y.Q., Zhou, K., 2020. Design and additive manufacturing of novel conformal cooling molds. Materials & Design, 196.

Torres-Alba, A., Mercado-Colmenero, J.M., de D. Caballero-Garcia, J., Martin-Doñate, C., 2021. Application of New Triple Hook-Shaped Conformal Cooling Channels for Cores and Sliders in Injection Molding to Reduce Residual Stress and Warping in Complex Plastic Optical Parts. Polymers, 13.

Torres-Alba, A., Mercado-Colmenero, J.M., Diaz-Perete, D., Martin-Doñate, C., 2020. A New Conformal Cooling Design Procedure for Injection Molding Based on Temperature Clusters and Multidimensional Discrete Models. Polymers, 12.

Wang, Y., Yu, K.M.,. Wang. C.C.L, Zhang, Y., 2011. Automatic design of conformal cooling circuits for rapid tooling. Computer-Aided Design, 43(8), 1001-1010.

Wang, Y., Yu, M.K., Wang, C.C.L., 2015. Spiral and conformal cooling in plastic injection molding. Computer-Aided Design, 63, 1-11.

Wang, Y., Yu, M.K., Wang, C.C.L., Zhang, Y., 2011. Automatic design of conformal cooling circuits for rapid tooling. Computer-Aided Design, 43(8), 1001-1010.
Wu, T., Jahan, S.A., Kumaar, P., Tovar, A., El-Mounayri, H., Zhang, Y., Zhang, J., Acheson, D., Brand, K., Nalim, R., 2015. A Framework for Optimizing the Design of Injection Molds with Conformla Cooling for Additice Manufacturing. Procedia Manufactruing, 404-415.
Wu, T., Tovar, A., 2018. Design for Additive Manufacturing of Conformal Cooling Channels Using Thermal-Fluid Topology Optimization and Application in Injection Molds. Proceedings of the ASME 2018 International Design Engineering Technical Conferences & Computers and Information in Engineering Conference. Quebec City, Canada.
Xu, X., Sach, E., Allen, S., 2004. The Design of Conformal Cooling Channels in Injection Moulding Tooling. Polymer Engineering and Science, 41(7), 1265-1279.
Yasa, E., Poyraz, O., Cizioglu, N., Pilatin, S., 2015. Repair and Manufacturing of High Performance Tools by Additive Manufacturing. 8th International Conference and Exhibition on Design and Production of MACHINES and DIES/MOLDS. Kusadasi, Aydin, TURKEY.
Zhang, Y.M., Hou, B.K., Wang, Q., Li, Y., Huang, Z.G., 2017. Automatic design of conformal cooling channels in injection molding tooling. International Conference on Mechanical Engineering and Applied Composite Materials. Hong Kong.

## Appendix

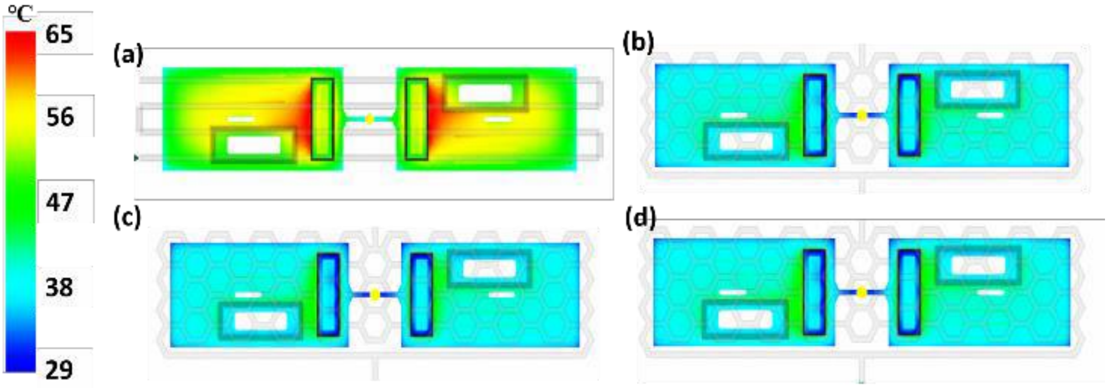


**Fig. 12.** Temperature results for (a) SCC, (b) OC, (c) FC, (d) HC

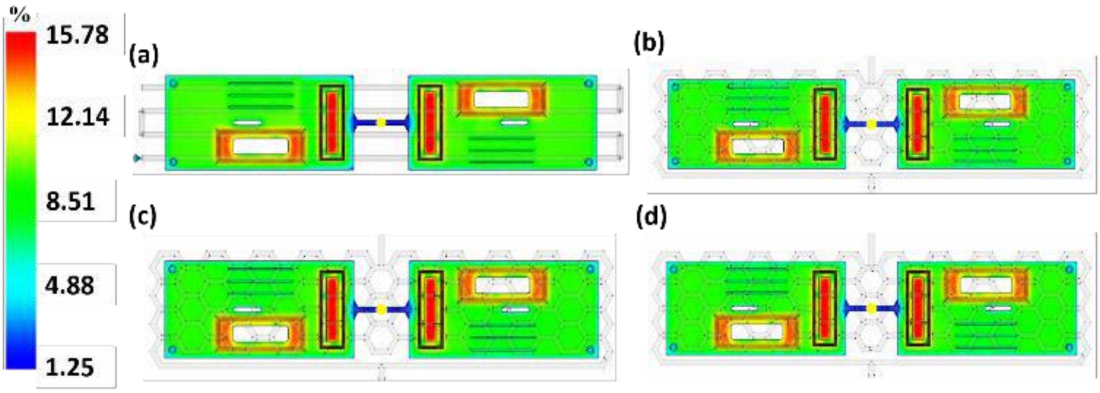


**Fig. 13.** Volumetric shrinkage results for (a) SCC, (b) OC, (c) FC, (d) HC

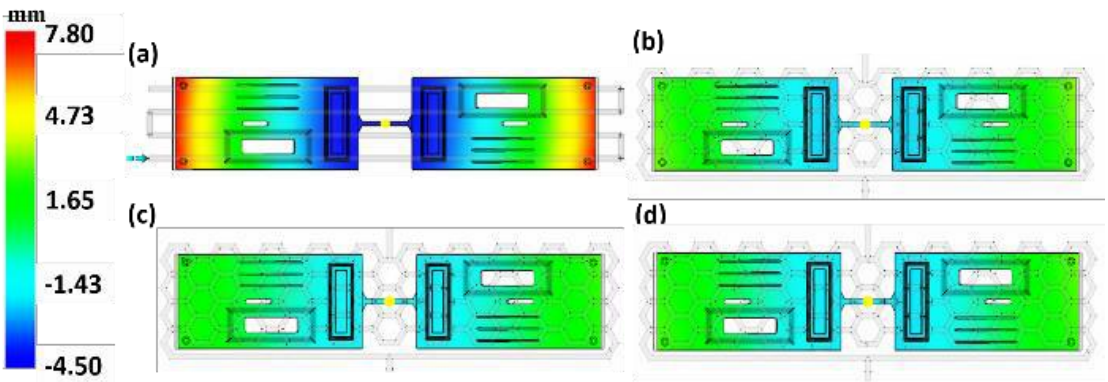


**Fig. 14.** Warpage results for (a) SCC, (b) OC, (c) FC, (d) HC

# 用于提高注塑成型质量的蜂窝随形冷却通道的自动化设计

**關鍵詞**
随形冷却通道
自动构建
一模多腔
冷流道系统
蜂窝

**摘要**
随形冷却通道的研究通常在模型设计中采用两个假设：使用 (1) 热流道系统和 (2) 一模一腔设计。 这些假设大大简化了研究。 然而，大多数模具都是使用冷流道系统和多个型腔设计的。 这两个假设可能不适用于所有商业系统； 因此，本研究提出了一种用于冷流道系统和多腔的蜂窝 CCC 的设计方法。 具体来说，开发了一种算法来自动为此类系统设计 CCC。 该算法可用于减少冷却时间，提高产品质量，并确保实际情况下系统温度相对均匀。 根据这项研究的结果，蜂窝 CCC 模型在保持均匀的温度分布、减少收缩和减少由同一双腔模具生产的两个零件的翘曲方面更有效，从而确保一致的零件质量。